



Seismic Performance Assessment of Sustainable Shelter Building Using Microtremor Method

Rusnardi Rahmat Putra ^{1*}, Junji Kiyono ², Yusuke Ono ³, Dezy Saputra ¹

¹ Department of Civil Engineering, Universitas Negeri Padang, Sumatera Barat 25131, Indonesia.

² Graduate School of Engineering, Kyoto University, Kyoto, 615-8246, Japan.

³ Faculty of Engineering, Tottori University, 4-101, Koyama-Minami, Tottori, 680-8552, Japan.

Received 30 August 2024; Revised 14 October 2024; Accepted 21 October 2024; Published 01 November 2024

Abstract

The increasing intensity of earthquakes in West Sumatra could trigger megathrust earthquakes and tsunamis at the inter-plate in the Mentawai Islands. Building assessments are necessary to determine their vulnerability to predicted earthquakes. The target is a four-story building that serves as an education building and vertical evacuation. This research proposes a complete vulnerability assessment method using single microtremor observations, and the results are used to determine seismic building performance. The natural frequency is derived from the spectral analysis of the horizontal components (NS and EW) for each level, and we considered the largest earthquake peak ground motion (PGA) in this region to be the September 30, 2009, Padang earthquake (PGA 380 gals as ground motion input). We calculated the resonance index, seismic vulnerability index, and damping ratio. The results show that the resonance index of the structure is less than 1, the vulnerability index of the UNP Faculty of Economics building $\alpha > (1/100-1/200)$ and is 1/234 to 1/699 for the x direction and 1/207 to 1/709 for the y direction; the average damping ratio is <5% for both directions (x, y) and RDM and FSR relationship is 0.78 and 0.69 for x and y respectively. The overall findings indicate that the structural response of the evaluated buildings falls within the 'slight' damage category during seismic events.

Keywords: Vulnerability Assessment; Seismic Wave; Microtremor Single; Vulnerability Index; Building Resonance.

1. Introduction

Indonesia is situated at the convergence of three major tectonic plates: the Indo-Australian plate lies westward, the Pacific plate is eastward, and the Philippines plate lies northeast of Indonesia [1]. The movement of these plates results in a shift of 7 mm per year for the Indo-Australian plate in the western part of Indonesia, while the Pacific plate moves at a rate of 12 mm per year in the eastern region [2]. These tectonic activities highlight ongoing subduction beneath the region, including the Indonesian archipelago. Consequently, this increases earthquake occurrences, with approximately 1,200 yearly seismic events, most of which register above a magnitude of 4 on the Richter scale and occur at shallow depths [3]. West Sumatra, located in western Indonesia, is particularly prone to these events.

West Sumatra, geographically positioned near two major earthquake sources, has a history of large-scale seismic events. Fault lines traverse the region, passing through Singkarak, Padang Panjang, Padang, and Painan. Historical data from 1779 to 2020 shows that many earthquakes in this area have been of large magnitudes, including the 1928 (Mw 8.4), 1933 (Mw 9.3), 1981 (Mw 8.1), and 2007 (Mw 8.4) earthquakes. This data underscores the region's vulnerability

* Corresponding author: rusnardi.rahmat@ft.unp.ac.id

<http://dx.doi.org/10.28991/CEJ-2024-010-11-06>



© 2024 by the authors. Licensee C.E.J, Tehran, Iran. This article is an open access article distributed under the terms and conditions of the Creative Commons Attribution (CC-BY) license (<http://creativecommons.org/licenses/by/4.0/>).

to seismic events, which also pose tsunami risks, particularly those caused by underwater subduction, such as 1833 (Mw 9.2), 2005 (Mw 9.3), and most recently, the 2010 Mentawai earthquake (Figure 1).

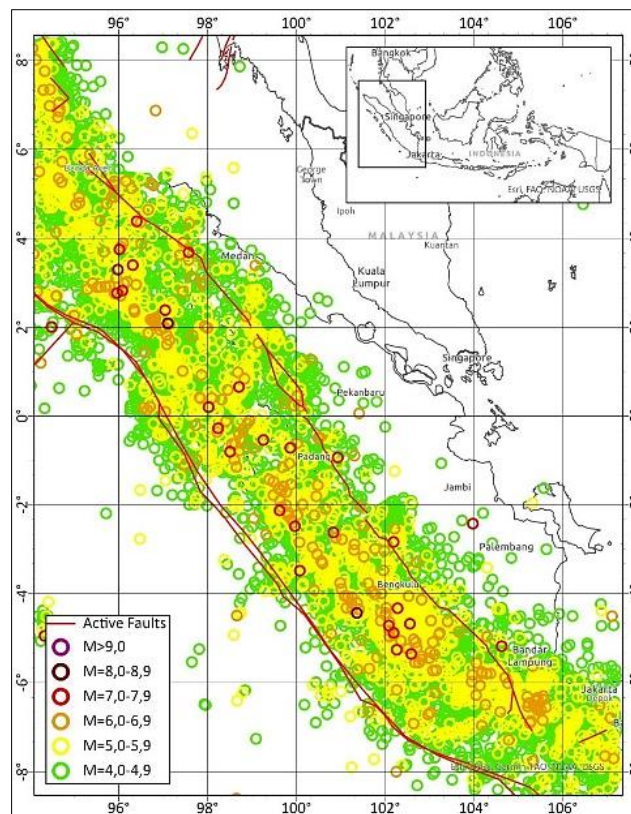


Figure 1. A fault line along the island of Sumatra (red line) and its slip rate [2]

The 2010 earthquake devastated West Sumatra with a magnitude of 7.6 on the Richter scale. It led to 1117 deaths, left two individuals missing, and caused 1214 serious injuries and 1688 minor injuries. The disaster also resulted in extensive damage to houses: 114,797 were heavily damaged and collapsed, 67,198 were moderately damaged, and 67,838 others were slightly damaged. In addition, several buildings and community infrastructures were destroyed, including 9432 public buildings and 42 government offices, 4748 educational facilities, 153 health facilities, 68 bridges, and 2851 places of worship [4]. Mitigation continues, with local governments conducting building vulnerability assessments since 2019. They will continue to be carried out for all the buildings used as vertical evacuations. The team has assessed several buildings with unsatisfying results. It is predicted that several buildings will be prone to collapse if earthquakes occur in the future [5,6].

Indonesia ranks among the countries with the most significant number of people exposed to tsunami hazards globally, with around 5.5 million individuals vulnerable to a tsunami event expected once every 500 years [6]. Between 1674 and 2018, Indonesia experienced 109 tsunamis, 98 of which were triggered by earthquakes, while 10 resulted from volcanic activity [7].

In the past decade, Indonesia has experienced several tsunamis, including the 2010 Mentawai tsunami, the 2018 Central Sulawesi tsunami, and the 2018 Sunda Strait tsunami. These events triggered landslides and liquefaction, resulting in casualties and extensive damage to the infrastructure. [8-10]. The hazard curve for Western Indonesia indicates the average tsunami risks for Sumatra and Java are comparable. However, the broader spread of Sumatra's hazard curves reflects its geographic position, with some areas located along the eastern coast of the Mentawai and Nias islands. The maximum anticipated tsunami height exceeds 9 meters along the coast of Mentawai Island and 5 meters along Sumatra's coast. [11, 12]. In Eastern Indonesia, the tsunami hazard curves for the Banda, Papua, and Sulawesi exhibit similar patterns. Thus, Western and Eastern Indonesia face high annual exceedance rates for potential tsunami hazards [13, 14]. Since earthquakes can potentially trigger tsunamis, the government must establish shelters for vertical evacuation. Around 65 buildings have been designated for this purpose, but their seismic performance remains uncertain.

Investigating the performance of several soil characteristics such as shear wave velocity, 30 m (VS30) and the predominant period of the site, and horizontal to vertical spectra ratio as estimators of seismic site effects for the target sites, soil characteristics significantly influence seismic building performance, primarily through its mechanical properties and the effectiveness of stabilization techniques [15, 16] conducted a rapid seismic assessment of an existing

building by using the methodology of PERA 19 based on actual damage due to the largest Turkey –Syria earthquake event in 2023. The method of PERA 19 is for building up ten stories, dimensions, cross-section of the column, slab, detail of transverse, and ratio of longitudinal reinforcement of each story. The single microtremor observation method is one of the fastest, most reliable, and most straightforward methods to identify dynamic soil properties related to seismic building performance [14, 17] conducted dynamic soil investigation and seismic building assessment for fourteen 2-4 stories building in Slovenia using microtremor results to determine the danger of soil-structure resonance. Single microtremor measurements were performed to understand the seismic behaviour of the building and the vulnerability of the swerved tower and compare it with other straight towers. The study showed that microtremor single measurement is a precise and reliable method for evaluating seismic performance and dynamic characteristics of the structural and vulnerability index of the targeted building [18].

This study aims to comprehensively evaluate these existing reinforced concrete (RC) structures by considering soil characteristics and seismic building performance derived from microtremor measurements and simulating the largest ground motion acceleration as a ground motion input.

2. Research Methodology

To analyze the dynamic behaviour and seismic performance of buildings, key parameters include natural frequency [14, 19], damping ratio [20, 21], and vulnerability index [22, 23]. These parameters can be obtained from ambient noise recordings within the building structure [24]. Determining the predominant frequency of a structure is particularly significant for studying resonance phenomena [14, 21]. The vulnerability index, which reflects the susceptibility of a structure to earthquake damage, can be estimated using the drift angle and related seismic acceleration inputs [24]. The seismic vulnerability index (K_a) is influenced by the dynamic characteristics of the soil, making it a crucial factor in evaluating structural vulnerability [14, 19]. For seismic assessments of existing buildings using the seismic index method, based on Japanese standards, the basic seismic index is determined by considering strength and flexibility criteria [25].

The current study considers both parameters, such as the natural frequency for each floor, and considers them to obtain resonance index, vulnerability index and damping ratio. The building selected for assessment is crucial for evacuation during earthquake and tsunami disasters. This building is located less than a kilometer offshore and in the red zone, prone to earthquakes. Soft soil is characterized by a V_{s30} value of less than 150 m/s^2 and a predominant period exceeding 1 second (Figure 2) [25, 26]. This research aims to thoroughly assess existing reinforced concrete (RC) buildings by incorporating essential structural and soil attributes, such as the predominant period and V_{s30} values derived from microtremor observations.

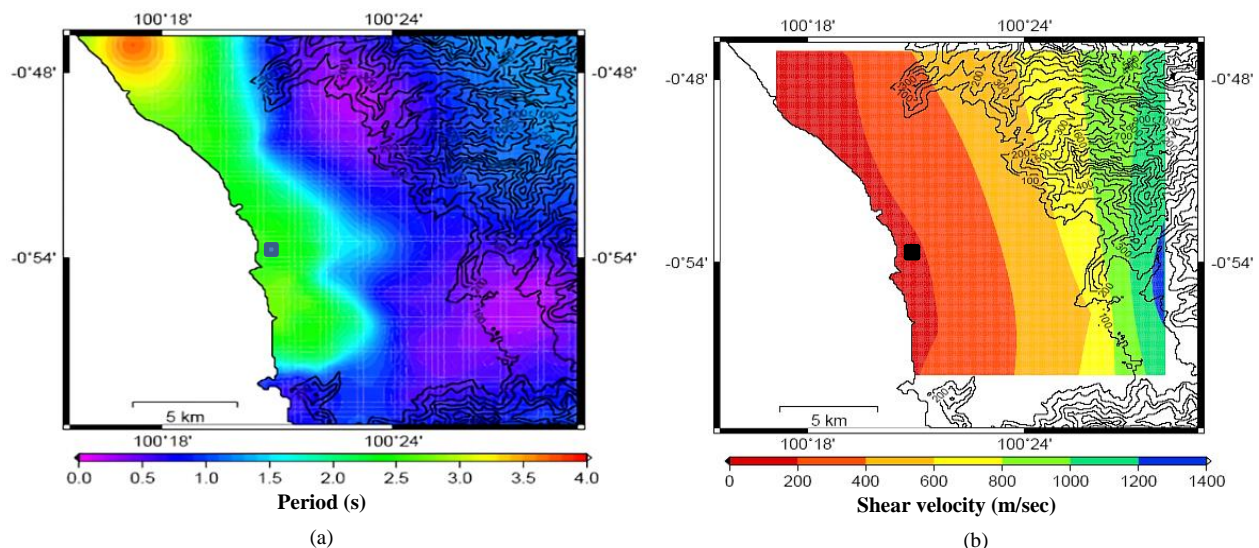


Figure 2. Building target location show in black box (a) H/V Ratio across Padang City and, (b) V_{s30} distribution across the entire Padang City

The population density around this building is $902 \text{ families/km}^2$, with 46,000 students at UNP. The selected building has four stories and is used for lectures at the Faculty of Economics, Padang State University. It was built in 2008 and used as a shelter for two major earthquakes: the Padang earthquake in 2019 and a significant earthquake and tsunami in the Mentawai Islands in 2010.

The building assessment was carried out in July 2023. built-in 2008 and used as a shelter for two significant earthquake events: the Padang earthquake in 2019 and a significant earthquake and tsunami in the Mentawai Islands in

2010. The building assessment was carried out in July 2023, built in 2008 and used as a shelter for two significant earthquake events: the Padang earthquake in 2019 and a significant earthquake and tsunami in the Mentawai Islands in 2010.

The instrument used was a GPL-6A3P microtremor with three direction sensors; the assessment was of 10 minutes duration and 200 Hz sampling frequency. Wave data retrieval was carried out twice on the ground and on each floor, from the 1st to the 4th floors, and in the x, y, and z directions. The outline of the selected building is shown in Table 1, and the building site plan and used device and research flow are shown in Figures 3 to 5, respectively.

Table 1. The Selected Building Characteristics

Component Type	Description
Usage	Education building
Number of stories	four
Building height	17.4 m
Structural type	R.C. Framed Structure
Foundation type	Shallow
Building area	2578.25 m ²
Total floor area	8788.6 m ²
Year of design	2005
Year of construction	Started 2006 and completed 2009
Concrete Strength	FC = 41.72 MPa
Re-bar Yield Strength	360 MPa
(Design)	Soil (Vs30 <150 m/s)
Soil type	17.4 m

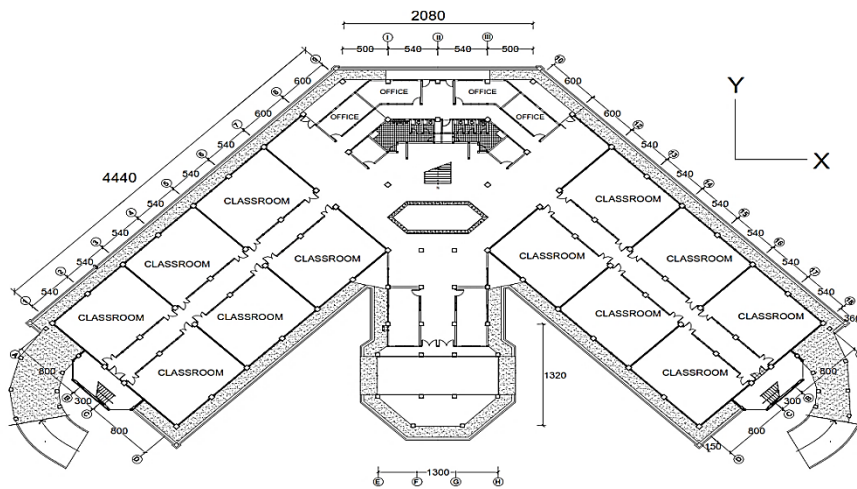


Figure 3. The site plan of the selected building and the red box represents the installed sensor location for each floor



Figure 4. The microtremor measuring instrument

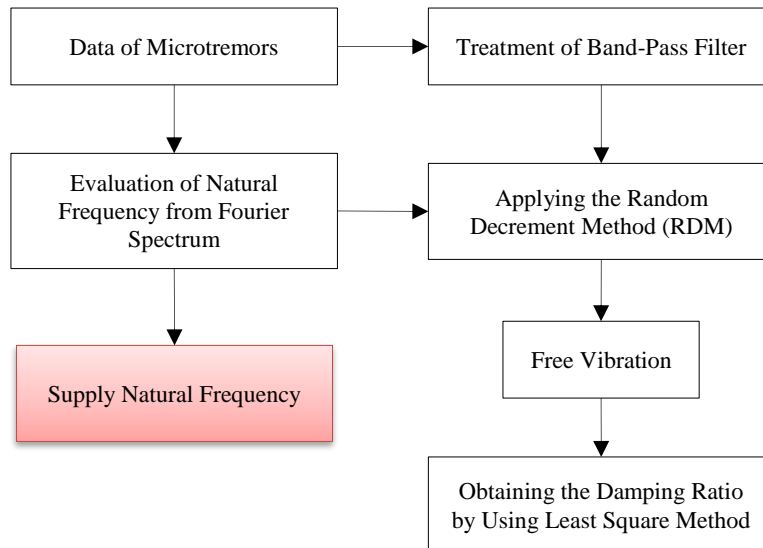


Figure 5. Research Flowchart

Using a microtremor observation result, we obtained the HVSR for the ground surface and the natural frequency from the 1st to the 4th floor for the horizontal direction (x, y). The recorded data included x, y, and z neural waveforms. For data analysis, the Horizontal-to-Vertical Spectral Ratio (HVSR) was determined at the ground level of the chosen building. The HVSR technique estimates the ratio of the Fourier amplitude spectra for the horizontal (H) and vertical (V) components of ambient noise measured at a single observation point (Equation 1) [21, 22]. The **HVSR** peak period is the predominant resonance correspondence period of the survey site.

$$HVSR = \sqrt{\frac{F_{NSi}(\omega)^2 + F_{EWi}(\omega)^2}{F_{UDi}(\omega)^2}} \tag{1}$$

Here $F_{NSi}(\omega)$ and $F_{EWi}(\omega)$ represent the Fourier amplitude of the North-South (NS_i), East-West (EW_i), and Up-Down (UD_i) components of each interval, respectively, and ω indicates the frequency. The frequency of this **HVSR** was used as the natural frequency of the ground surface. Meanwhile, the seismic waveform was obtained from single microtremor observations and converted to a frequency domain using Fourier analysis [22]. Since the predominant frequency of the building structure from the HVSR is not recommended for vulnerability assessment at the 2nd, 3rd, and 4th floors [23], measurements were repeated twice at each observation point for floor spectra ratio (FSR). To obtain the FSR of each floor is to use the spectra (EW and NS) of ambient noise in the building and the spectral ratio between the upper floor and basement (free field near the building) were analyzed for both components [14].

2.1. Building Resonance Ratio

Vulnerability is based on the building's resonance index. The susceptibility of a building to earthquakes is assessed using its resonance index and vulnerability index values [20, 21]. The following equation determines the building resonance ratio (R):

$$R = \frac{T_b}{T_s} < 1 \tag{2}$$

where T_b indicates the natural period of the building and T_s refers to the natural period of the ground surface. The resonance index classification suggests that a building is categorized as low resonance if R is less than 1. Conversely, when R is equal to or exceeds 1 (indicating that the building's natural period matches or surpasses that of the ground), the structure is at a higher risk for earthquake resonance, potentially resulting in damage. In this study, we used the natural period of the ground surface and building to calculate the resonance ratio.

2.2. Vulnerability Index

A drift angle can assess vulnerability according to the building structure's vulnerability index concerning earthquakes. The value of the building vulnerability index K_b is determined using the equation established by Nakamura et al. [23]. Another earthquake parameter is acceleration in cm/s^2 . Then, α is the effect of the structure during earthquake vibrations.

$$\alpha = ea \tag{3}$$

where e denotes the effectiveness of the earthquake ground motion impacting the structure. The structural deformation performance and the level of amplification due to earthquake motion can be assessed based on the building's dynamic

characteristics. In this research, the building's natural frequency is anticipated to determine the extent of damage incurred. Significant displacement of δ_i for each floor is estimated using the primary natural frequency and amplitude for each level, as outlined below:

$$\delta_i = \frac{A_i \alpha}{(2\pi F)^2} \quad (4)$$

Therefore, the drift angle δ_i of the i th floor is expressed as follows:

$$\gamma_i = \frac{\delta_{(i+1)} - \delta_i}{h} \quad (5)$$

$$= \Delta A_i \frac{\alpha}{(2\pi F)^2 h_i} 10^4 \quad (6)$$

$$= e K_{bi} a \quad (7)$$

where:

$$K_{bi} = \frac{\Delta A_i}{(2\pi F)^2 h_i} 10^4 \quad (8)$$

$$\Delta A_i = A_{i+1} - A_1 \quad (9)$$

ΔA_i represents the amplification difference on each floor, H_i denotes the height of each floor (in meters), and F indicates the predominant frequency of the building structure. Consequently, the drift angle γ_i is determined by multiplying the vulnerability index by the maximum acceleration of earthquake vibrations measured at ground level (in cm/s^2) for each level. We applied the region's most significant ground motion acceleration in the last 200 years (the September 30, 2009, Padang earthquake) and the efficiency of earthquake motion. This relationship is expressed in the following equation:

$${}_{av}K_{bi} = \frac{A 10^4}{(2\pi f)^2 H} \quad (10)$$

The maximum allowable acceleration from the column (Gals) is derived from Equation 6:

$$\alpha_i = 10^4 \frac{(2\pi F)^2 h_i}{\Delta A_i} \gamma_i \quad (11)$$

$$\alpha_i = 10^4 \frac{(2\pi F)^2 h_i}{\Delta A_i} \gamma_i \quad (12)$$

When ${}_{av}K_{bi}$ is substituted for Equation 3, H represents the overall height of the building structure and the average drift angle-subscript base, angle δ_{av} a be computed. The values of K_{bi} and ${}_{av}K_{bi}$ represented in units of 10,000 as illustrated in Equations 3 and 4.

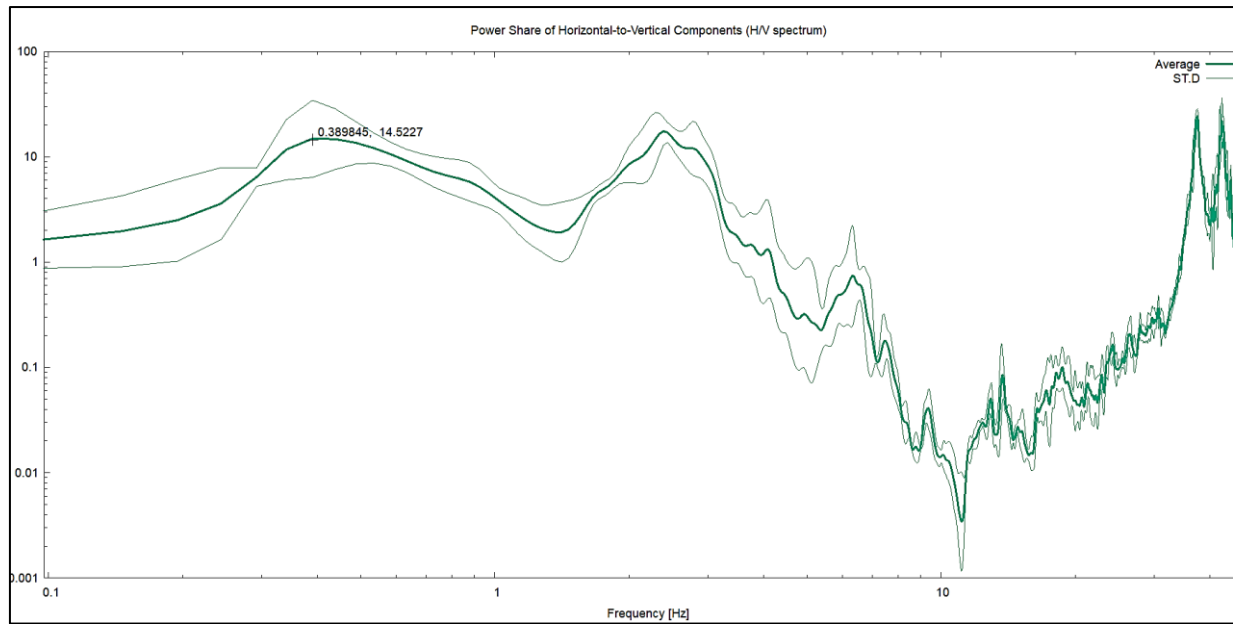
In this research, microtremor measurements were conducted for each floor. **HVSR** results for the bottom (ground) and predominant period from FFT (Fast Fourier Transform) analyze the results for the 1st, 2nd, 3rd, and 4th floors. The value of the drift angle is also determined by the prediction of earthquake vibration acceleration and the effectiveness of the ground motion efficiency.

2.3. Damping Ratios Determined through RDM Technique

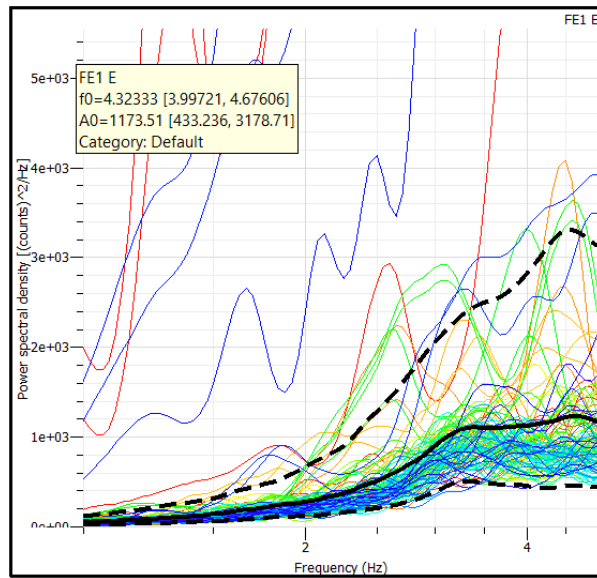
Determining the damping ratio is crucial for understanding how a structure dissipates earthquake energy. This parameter is valuable for assessing structural resilience against seismic forces and estimating structural vulnerability [24-27]. The damping ratios are determined using the RDM method, with a band-pass filter applied before RDM processing. The filter settings are adjusted according to the predominant frequency obtained through the FSR method. To compute the damping ratio, the structure's natural frequency must be known [23, 28]. Thus, the structure's spectrum and RDM should be analyzed concurrently.

3. Result and Discussion

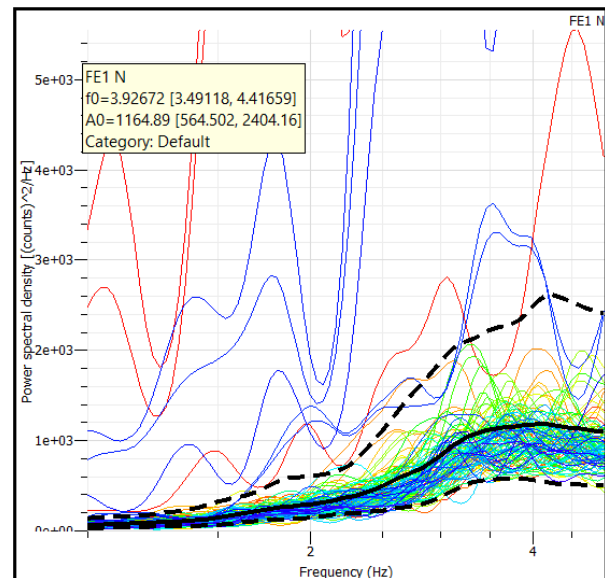
The HVSR resulted in a comparator or ground frequency (0.36 Hz) with a predominant period (2.75s) (Figure 6). It identified that the surface soil condition was soft and the predominant period of the soil was > 1 s [29, 30]. The building's average natural frequency is 4.01 Hz, with a predominant period of 0.249 seconds, as illustrated Figures 6-b and 6-c and Tables 2 and 3.



(a)



(b)



(c)

Figure 6. Natural frequency (a) ground floor and each floor for (b) for the x-direction and (c) y-direction

Table 2. Seismic vulnerability evaluation result for x direction

Floor	Height	Floor Spectral Ratio (FSR)							Random Decrement Method (RDM)	
		f_0 (Hz)	A	Kb	e	α	δ	γ	f_0 (Hz)	Z (%)
1	4	4.32	1.17	3.97	0.5	398	0.632677	0.00079	2.13	1.94
2	8	3.47	1.37	3.61	0.5	398	1.148221	0.00072	2.11	1.55
3	12	3.13	2.77	5.97	0.5	398	2.853349	0.00119	2.12	3.31
4	16	5.74	5.70	2.74	0.5	398	1.745882	0.00055	2.25	8.01

Table 3. Seismic vulnerability evaluation result for y direction

Floor	Height	Floor Spectral Ratio (FSR)							Random Decrement Method (RDM)	
		f_0 (Hz)	A	Kb	e	α	δ	γ	f_0 (Hz)	Z (%)
1	4	3.92	1.16	4.79	0.5	398	0.761815	0.00095	2.13	2.67
2	8	4.14	1.79	3.31	0.5	398	1.053941	0.00066	2.13	3.59
3	12	3.04	3.20	7.32	0.5	398	3.494352	0.00146	2.14	1.57
4	16	4.46	2.96	2.36	0.5	398	1.501709	0.00047	2.15	1.92

The obtained resonance index is 0.09 ($\ll 1$). A lower resonance index indicates that the building's natural frequency is nearly equal to the ground frequency. Therefore, it is more prone to experiencing earthquake resonance, which can cause damage to the building. From Equation 11, the maximum acceptable acceleration is about 398 Gals and γ_i can be as much as 1/400 (Table 2). Generally, the building will have a high risk of collapse if the drift angle is 1/100–1/200 [19]. The current vulnerability assessment approach, which utilizes *HVSR* for the ground level (1st floor) and the predominant frequency in the x, y, and z directions from FFT for the upper floors, proves effective. The natural frequency for each floor is 4.0 Hz in both the x and y directions, as illustrated in Figure 6-b. The average damping ratio is 3.74% for the x direction and 2.43% for the y direction (refer to Figure 7 and Tables 2 and 3)

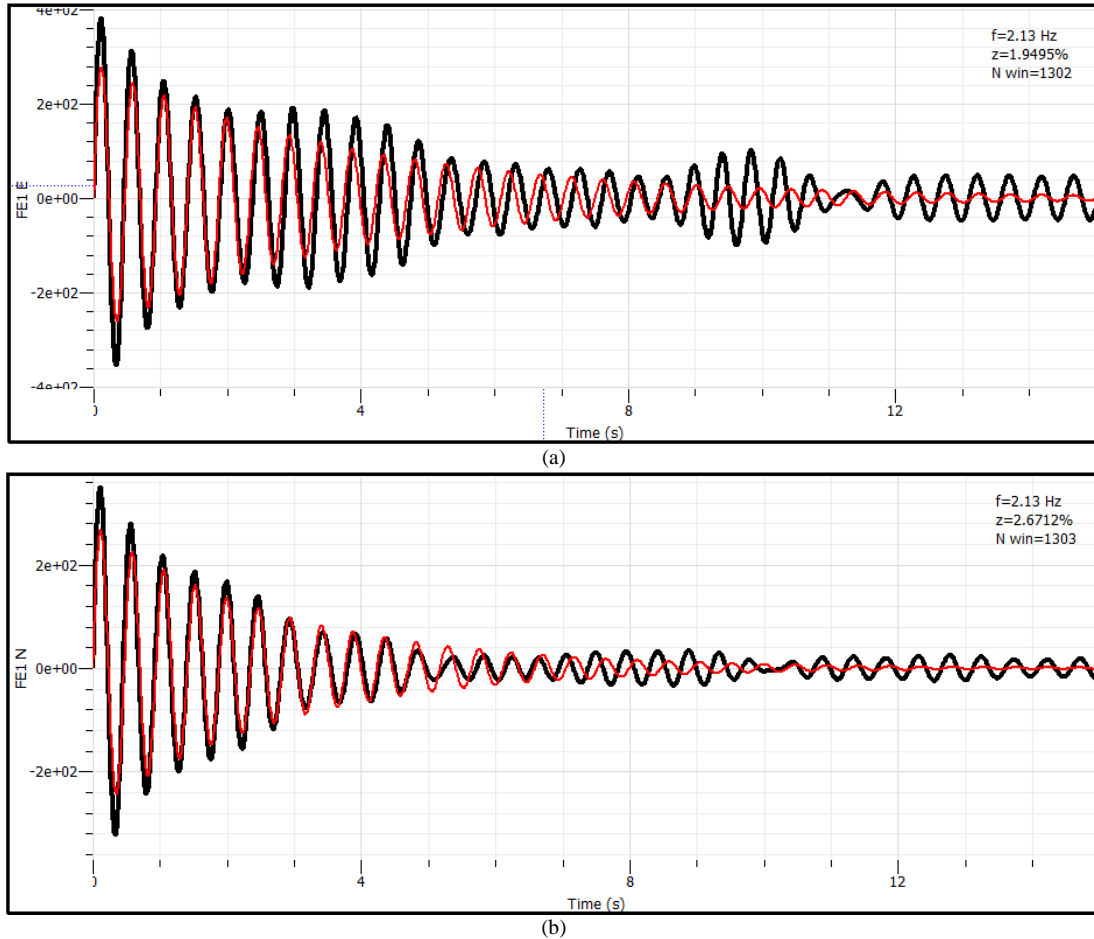


Figure 7. Sample of RDM Analysis for each floor (a) for x direction and (b) for y direction

Figure 8 displays the fundamental frequencies obtained through the RDM method, which closely align with those determined using the FSR technique, as indicated by the correlation coefficient ($R^2 = 0.69$) between the observed and predicted values. Therefore, reliability must be close to the damping ratio of the buildings and the natural frequencies resulting from FSR and RDM.

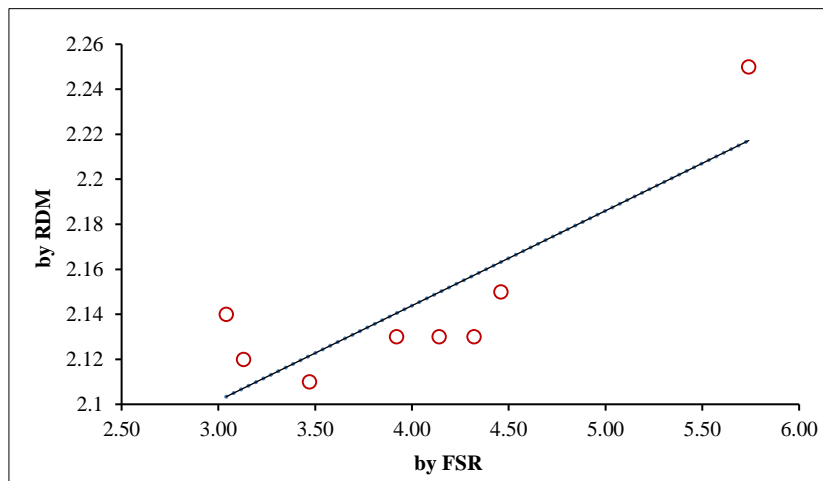


Figure 8. Comparison of Fundamental Frequencies Obtained Using RDM and FSR Methods

The frequency and damping ratio relationship reveals a similar structural and natural frequency trend. A model for this relationship was developed using robust regression, resulting in an R^2 value of 0.78, as illustrated in Figure 9. About the fitting curve shown in Figure 9, the damping ratio increases with increasing fundamental frequency [31, 32]. We assessed the target building as vertical evacuation for students and people who are living near this building to face the predicted earthquake in the future; the building is a 4-story building located offshore, less than 100m away, with soft soil (natural period of soil $>1s$) and $>10m$ of predicted inundation height. The structural response of the building during seismic events is a primary parameter to be considered in making a policy for a vertical evacuation building [33, 34]. The current study applied a complete seismic performance assessment parameter such as building resonance ratio and, vulnerability index and, floor spectra ratio, damping ratio of the building and used the most significant ground motion acceleration in this region (0.38g, September 30, 2009, Padang earthquake) as ground motion input. We consider both the FSR and damping ratios since the building's inherent frequency increases, and the damping ratio will increase, too [32].

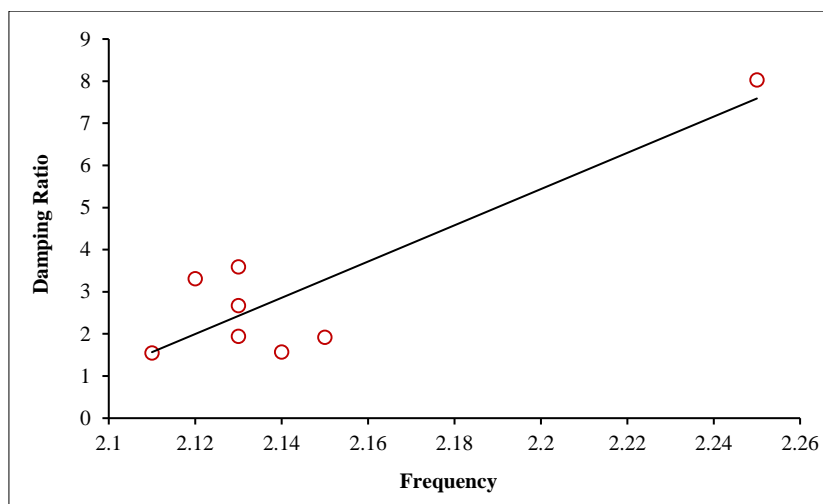


Figure 9. Relationship Between Damping Ratio and Fundamental Frequency of the Building Structure

The results indicate that the seismic performance of the target building falls within the slight damage category. We conducted a preliminary visual assessment of the selected building by applying the Japan Building Disaster Prevention Association seismic Evaluation and retrofit [35] each part of the building, such as columns, beams, and walls, due to the September 30, 2009, Padang earthquake just one month after the quake. We found cracks in some area walls (non-structural); fortunately, there was no severe damage in the structural part of this building [25]. Finally, we categorized the selected building as a slight category for preliminary visual assessment. The two results from seismic performance assessment using microtremor and visual damage assessment are similar. This classification aligns with the building's condition following the September 30, 2009, Padang earthquake only. The literature study found that measurements of microtremors in buildings are efficient and quick, with reliable, accurate results and estimates of the dynamical characteristics of the building structure and applicable methods to other buildings with different regions [36].

4. Conclusion

Measurements of microtremors in buildings are efficient and quick, with reliable, accurate results and estimates of the dynamical characteristics of the building structure. The damping ratios are determined using the RDM method, which is valuable for assessing structural resilience against seismic forces and estimating structural vulnerability [26]. This study considers the spectra (EW and NS) of ambient noise in the building for FSR and RDM for each floor and the spectral ratio between the upper floor and basement. The reliability must be close to the buildings' damping ratio and the natural frequencies resulting from FSR and RDM.

This study evaluates the selected building's dynamic characteristics and seismic vulnerability, which were assessed using microtremor measurements. The methods applied, including the Floor Spectral Ratio (FSR) and vulnerability calculations, are presented in Tables 2 and 3. The findings indicate that the building has a low vulnerability, with the drift angle (α) ranging from $1/234$ to $1/699$ for the x-direction and $1/207$ to $1/709$ for the y-direction. The peak ground acceleration (PGA) recorded during an earthquake was less than 398 Gals, placing it in the low-index category. The angle is $1/100$ – $1/200$. The current vulnerability assessment method is applicable, using HVSr for the ground (1st) floor and predominant frequency direction x, y, and z from FTT for $>$ of the 1st story. The natural frequency for each floor was measured at 4.0 Hz for both x and y directions, with average damping ratios of 3.74% and 2.43%, respectively. The building exhibits low resonance, with R-values below 1, indicating minimal risk of resonance. Overall, the results classify the building's seismic performance in the 'slight' damage category. From the overall results, the existing four-stories building, approximately 20m in height, is recommended for vertical evacuation.

5. Declarations

5.1. Author Contributions

Conceptualization, P.R.R., J.K., and Y.O.; methodology, P.R.R., J.K., and Y.O.; validation, P.R.R., J.K., and Y.O.; formal analysis, P.R.R., J.K., and Y.O.; investigation, P.R.R. and M.D.S.; resources, P.R.R. and M.D.S.; data curation, P.R.R. and M.D.S.; writing—original draft preparation, P.R.R., J.K., and Y.O.; visualization, P.R.R. and M.D.S.; supervision, P.R.R., J.K., and Y.O.; project administration, P.R.R. and M.D.S. All authors have read and agreed to the published version of the manuscript.

5.2. Data Availability Statement

The data presented in this study are available on request from the corresponding author.

5.3. Funding and Acknowledgments

The authors thank Darma Agung (BEng) and Rezqya (BEng) for their invaluable assistance in data collection. We are also grateful to Yusuke Ono from Tottori University, Japan, for his contributions to the data analysis. A special acknowledgement is given to the students whose efforts greatly supported the assessment process. Finally, we thank the World Class University (WCU) of UNP for providing financial support through the research grant under contract number 4931/UN35.13/KP/2022.

5.4. Conflicts of Interest

The authors declare no conflict of interest.

6. References

- [1] Hady, A. K., & Marliyani, Dr., G. I. (2021). Updated Segmentation Model and Cummulative Offset Measurement of the Aceh Segment of the Sumatran Fault System in West Sumatra, Indonesia. *Journal of Applied Geology*, 5(2), 84. doi:10.22146/jag.56134.
- [2] Natawidjaja, D. H. (2018). Major Bifurcations, Slip Rates, and A Creeping Segment of Sumatran Fault Zone in Tarutung-Sarulla-Sipirok-Padangsidempuan, Central Sumatra, Indonesia. *Indonesian Journal on Geoscience*, 5(2), 137–160. doi:10.17014/IJOG.5.2.137-160.
- [3] Putra, R. R., Kiyono, J., Ono, Y., & Parajuli, H. R. (2012). Seismic Hazard Analysis for Indonesia. *Journal of Natural Disaster Science*, 33(2), 59–70. doi:10.2328/jnds.33.59.
- [4] Putra, R. R., Kiyono, J., & Furukawa, A. (2014). Vulnerability assessment of non-engineered houses based on damage data of the 2009 padang earthquake in Padang city, Indonesia. *International Journal of GEOMATE*, 7(2), 1076–1083. doi:10.21660/2014.14.140714.
- [5] Widiyantoro, S., Gunawan, E., Muhari, A., Rawlinson, N., Mori, J., Hanifa, N. R., Susilo, S., Supendi, P., Shiddiqi, H. A., Nugraha, A. D., & Putra, H. E. (2020). Implications for megathrust earthquakes and tsunamis from seismic gaps south of Java Indonesia. *Scientific Reports*, 10(1). doi:10.1038/s41598-020-72142-z.
- [6] Harig, S., Immerz, A., Weniza, Griffin, J., Weber, B., Babeyko, A., Rakowsky, N., Hartanto, D., Nurokhim, A., Handayani, T., & Weber, R. (2020). The Tsunami Scenario Database of the Indonesia Tsunami Early Warning System (InaTEWS): Evolution of the Coverage and the Involved Modeling Approaches. *Pure and Applied Geophysics*, 177(3), 1379–1401. doi:10.1007/s00024-019-02305-1.
- [7] Hamzah, L., Puspito, N. T., & Imamura, F. (2000). Tsunami Catalog and Zones in Indonesia. *Journal of Natural Disaster Science*, 22(1), 25–43. doi:10.2328/jnds.22.25.
- [8] Echebba, E. M., Boubel, H., El Omari, A., Rougui, M., Chourak, M., & Chehade, F. H. (2021). Analysis of the Second Order Effect of the SSI on the Building during a Seismic Load. *Infrastructures*, 6(2), 20. doi:10.3390/infrastructures6020020.
- [9] Brune, S., Babeyko, A. Y., Gaedicke, C., & Ladage, S. (2010). Hazard assessment of underwater landslide-generated tsunamis: A case study in the Padang region, Indonesia. *Natural Hazards*, 53(2), 205–218. doi:10.1007/s11069-009-9424-x.
- [10] Aránguiz, R., Esteban, M., Takagi, H., Mikami, T., Takabatake, T., Gómez, M., González, J., Shibayama, T., Okuwaki, R., Yagi, Y., Shimizu, K., Achiari, H., Stolle, J., Robertson, I., Ohira, K., Nakamura, R., Nishida, Y., Krautwald, C., Goseberg, N., & Nistor, I. (2020). The 2018 Sulawesi tsunami in Palu city as a result of several landslides and coseismic tsunamis. *Coastal Engineering Journal*, 62(4), 445–459. doi:10.1080/21664250.2020.1780719.
- [11] Lange, D., Tilmann, F., Henstock, T., Rietbrock, A., Natawidjaja, D., & Kopp, H. (2018). Structure of the central Sumatran subduction zone revealed by local earthquake travel-time tomography using an amphibious network. *Solid Earth*, 9(4), 1035–1049. doi:10.5194/se-9-1035-2018.

- [12] Aydan, O. (2008). Seismic and tsunami hazard potentials in Indonesia with a special emphasis on Sumatra Island. *Journal of the School of Marine Science and Technology-Tokai University (Japan)*, 6(3), 19-38.
- [13] Thein, P. S., Pramumijoyo, S., Brotopuspito, K. S., Wilopo, W., Kiyono, J., Setianto, A., & Putra, R. R. (2015). Designed microtremor array based actual measurement and analysis of strong ground motion at Palu city, Indonesia. *AIP Conference Proceedings*, 1657, 040007. doi:10.1063/1.4915040.
- [14] Gosar, A. (2010). Site effects and soil-structure resonance study in the Kobarid basin (NW Slovenia) using microtremors. *Natural Hazards and Earth System Sciences*, 10(4), 761–772. doi:10.5194/nhess-10-761-2010.
- [15] Mercado, V., Díaz-Parra, F. J., Pajaro, C. A., Montejo, J., Posada, G., Arcila, M., & Arteta, C. A. (2024). Performance evaluation of parameters as estimators of seismic site effects in northern South America. *Soil Dynamics and Earthquake Engineering*, 180. doi:10.1016/j.soildyn.2024.108584.
- [16] Aydogdu, H. H., & Ilki, A. (2024). Case study for a performance based rapid seismic assessment methodology (PERA2019) based on actual earthquake damages. *Bulletin of Earthquake Engineering*, 22(4), 1965–1999. doi:10.1007/s10518-023-01841-5.
- [17] Karsli, F., & Bayrak, E. (2024). Single-station microtremor surveys for site characterization: A case study in Erzurum city, eastern Turkey. *Earthquake Engineering and Engineering Vibration*, 23(3), 563–576. doi:10.1007/s11803-024-2257-5.
- [18] Lantada, N., Pujades, L. G., & Barbat, A. H. (2009). Vulnerability index and capacity spectrum based methods for urban seismic risk evaluation. A comparison. *Natural Hazards*, 51, 501-524. doi:10.1007/s11069-007-9212-4.
- [19] Akkaya, İ. (2020). Availability of seismic vulnerability index (K_g) in the assessment of building damage in Van, Eastern Turkey. *Earthquake Engineering and Engineering Vibration*, 19(1), 189–204. doi:10.1007/s11803-020-0556-z.
- [20] Cole, H. A. (1973). *On-Line Failure Detection and Damping Measurement of Aerospace Structures by Random Decrement Signatures*. NASSA CR 2205, Elsen Engineering and Research, Inc., Mountain View, United States.
- [21] Herak, M. (2011). Overview of recent ambient noise measurements in Croatia in free-field and in buildings. *Geofizika*, 28(1), 21–40.
- [22] Farsi, M. N., Chatelain, J. L., Guillier, B., & Bouchelouh, A. (2010). Evaluation of the quality of repairing and strengthening of buildings. *Proceedings of the 14th ECEE*, 30 August- 3 September, 2010, Ohrid, Republic of Macedonia.
- [23] Nakamura, Y., Gurler, E. D., Saita, J., Rovelli, A., & Donati, S. (2000). Vulnerability investigation of Roman Colosseum using microtremor. *12th World Conference on Earthquake Engineering*, 30 January- 4 February, 2000, Auckland, New Zealand.
- [24] Sato, T., Nakamura, Y., & Saita, J. (2008). The change of the dynamic characteristics using microtremor. *The 14th World Conference on Earthquake Engineering*, 12-17 October, 2008, Beijing, China.
- [25] Putra, R. R., Ono, Y., Syah, N., & Cantika, A. A. (2021). Seismic performance evaluation of existing building in earthquake prone area based on seismic index and seismic demand method. *Civil Engineering and Architecture*, 9(4), 1237–1245. doi:10.13189/cea.2021.090425.
- [26] Mucciarelli, M., Herak, M., & Cassidy, J. (2008). Increasing seismic safety by combining engineering technologies and seismological data. *Proceedings of the NATO Advanced Research Workshop on Increasing Seismic Safety by Combining Engineering Technologies and Seismological Data*, 19-21 September, 2007, Dubrovnik, Croatia.
- [27] Crisci, G., Gentile, R., Ceroni, F., Galasso, C., & Lignola, G. P. (2024). Seismic vulnerability assessment of RC deck-stiffened arch bridges. *Engineering Structures*, 317, 118595. doi:10.1016/j.engstruct.2024.118595.
- [28] Mache, A., Kulkarni, A., Shah, S., Gujar, A., & Hujare, P. (2024). Exploring Natural Frequency and Damping in Coir-Rubber Polymer Composites for Vibration Control in Mobility Vehicles. *SAE Technical Papers*. doi:10.4271/2024-01-2357.
- [29] Hakimi, B., Masoumi, Z., Ghods, A., & Etemad-Saeed, N. (2019). Microtremor HVSR study of site effects in Zanjan city (Iran). *Iranian Journal of Geophysics*, 12(4), 115–139.
- [30] Petersen, M. D., Shumway, A. M., Powers, P. M., Mueller, C. S., Moschetti, M. P., Frankel, A. D., Rezaeian, S., McNamara, D. E., Luco, N., Boyd, O. S., Rukstales, K. S., Jaiswal, K. S., Thompson, E. M., Hoover, S. M., Clayton, B. S., Field, E. H., & Zeng, Y. (2021). The 2018 update of the US National Seismic Hazard Model: Where, why, and how much probabilistic ground motion maps changed. *Earthquake Spectra*, 37(2), 959–987. doi:10.1177/8755293020988016.
- [31] Zhang, Z., & Cho, C. (2009). Experimental study on damping ratios of in-situ buildings. *International Journal of Engineering and Applied Sciences*, 5(4), 264-268.
- [32] Dunand, F., Bard, P. Y., Chatelain, J. L., Guéguen, P., Vassail, T., & Farsi M. N. (2002) Damping and frequency from RANDOMDEC method applied to in situ measurements of ambient vibrations. Evidence for effective soil structure interaction. *The 12th European Conference on Earthquake Engineering*, 9-13 September 2002, London, United Kingdom.

- [33] ICC. (2024). International Code (IBC2024). International Code Council (ICC), Washington, United States.
- [34] El-Betar, S. A. (2017). Seismic performance of existing R.C. framed buildings. *HBRC Journal*, 13(2), 171–180. doi:10.1016/j.hbrj.2015.06.001.
- [35] The Japan Building Disaster Prevention Association. (2001). *Seismic Evaluation and Retrofit*. The Japan Building Disaster Prevention Association, Tokyo, Japan.
- [36] Hadianfard, M. A., Rabiee, R., & Sarshad, A. (2017). Assessment of Vulnerability and Dynamic Characteristics of a Historical Building Using Microtremor Measurements. *International Journal of Civil Engineering*, 15(2), 175–183. doi:10.1007/s40999-016-0086-2.